



HAL
open science

Validation of the Space-Time Variability of African Easterly Waves Simulated by the CNRM GCM.

Céron J.-P., Guérémy J.-F.

► **To cite this version:**

Céron J.-P., Guérémy J.-F.. Validation of the Space-Time Variability of African Easterly Waves Simulated by the CNRM GCM.. *Journal of Climate*, 1999, 12 (9), pp. 1022-1032. 10.1175/1520-0442(1999)0122.0.CO;2 . meteo-00374979

HAL Id: meteo-00374979

<https://meteofrance.hal.science/meteo-00374979>

Submitted on 8 Feb 2021

HAL is a multi-disciplinary open access archive for the deposit and dissemination of scientific research documents, whether they are published or not. The documents may come from teaching and research institutions in France or abroad, or from public or private research centers.

L'archive ouverte pluridisciplinaire **HAL**, est destinée au dépôt et à la diffusion de documents scientifiques de niveau recherche, publiés ou non, émanant des établissements d'enseignement et de recherche français ou étrangers, des laboratoires publics ou privés.

usually associated with larger vorticity anomalies at low levels but is limited in height at around 600 hPa, notably in terms of the vertical velocity field; the wave axis tilts eastward (westward) with height below (above) the AEJ (Reed et al. 1977). The southerly component of the AEWs has a deeper structure with a mid- to upper-tropospheric level maximum in the vertical velocity field; the wave axis tilts in the same direction as for the northerly component, the tilt being less (more) pronounced below (above) the AEJ (Reed et al. 1977). Due to these two components, two preferred tracks of vorticity maximum (used as a marker of the AEWs) do exist over the African continent at low levels, one located between 8° and 15°N and a second one located between 17° and 25°N. The southerly component has been the most extensively studied (due to the availability of observations and an apparent relationship between precipitation and possible generation of tropical cyclones). The observational studies referred to above have shown that the southerly component of the waves forms somewhere between 20°E and 0° and reaches its largest amplitude around the west coast of Africa with the maximum development occurring between 10°E and the west coast (Albignat and Reed 1980). This southerly component generally decays over the ocean, but it can also regenerate into tropical cyclones. The northerly component forms between 10°E and 10°W and reaches its largest amplitude near the west coast; most of the time it turns southward and generally decays over the ocean, tending to merge with the southerly component (Nitta and Takayabu 1985; Reed et al. 1988b). From GATE studies, it appeared that the waves have a wavelength of between 2000 and 3000 km, a period of 3 to 5 days, and therefore a westward phase speed of about 7 m s⁻¹.

The association of convective activity and precipitation with the waves has been studied for many years; but with the availability of satellite observations, it became possible to merge the satellite pictures with meteorological analyses to visualize a continuous space-time evolution of the interaction between the waves and the clouds. There is a maximum of rainfall and cloud cover ahead (behind) of the trough axis for the southerly (northerly when clouds do occur) component of AEWs (Carlson 1969a; Reed et al. 1977). Payne and McGarry (1977) presented similar results (using the GATE dataset for the southerly waves) for large cloud clusters but showed that smaller clusters occurred most frequently near the ridge axis; in particular, squall lines seemed to appear preferably ahead of the wave trough. Duvel (1990) has shown that the largest deep convective activity is located at and ahead of the trough around 8°N during the years 1983–85. But around 18°N the deep convection has a primary maximum east of the trough. Finally, Toledo Machado et al. (1993) have shown that the largest size clusters appear at and ahead of the wave trough when the wave amplitude is the largest.

Concerning our understanding of the physical mech-

anisms involved in the life cycle of the waves, several papers have been published so far. The main results on this topic were presented after GATE. A comprehensive study of the energetics of the waves was carried out by Norquist et al. (1977), in which they showed that both barotropic and baroclinic conversions between the wave and the AEJ could explain a large part of the life cycle of the waves, the baroclinic conversion being the largest over land. The role of these dynamical instabilities of the AEJ in the life cycle of the AEWs explains the possible existence at the same time of two low-level vorticity maxima, on each side of the jet. The southerly component of the AEWs interacts very often with deep convection, which results in a deeper and quite different vertical structure than that of the northerly component (Reed et al. 1977). Several authors have conducted linear instability studies, using mainly observed data on the AEJ at 5°E (which is a location of mature waves), which have given unstable modes dominated by barotropic energy conversions (Rennick 1976; Mass 1979). More recently, Thorncroft and Hoskins (1994a) and Paradis et al. (1995) have published similar studies, but the inclusion of a simple cumulus parameterization seemed to increase the growth rate and favor the baroclinic conversion. Thorncroft and Hoskins (1994b) have shown that the nonlinear behavior of an easterly wave normal mode is dominated by a baroclinic conversion (except for the generation still dominated by a barotropic conversion), when both conditional instability of the second kind and boundary layer parameterizations were included.

A significant interannual variability in the amplitude and location of the waves does exist (Reed et al. 1988b). However, this topic has not been much addressed because of the lack of a long and continuous (in space and time) dataset.

There are only a few studies on simulated AEWs produced by primitive equation models including a comprehensive physics package. Walker and Rowntree (1977) have integrated a limited area model over 10 days, and they have shown that the maintenance of the wave eddy kinetic energy was mainly due to baroclinic conversion, once the wave formed. Estoque et al. (1983) have simulated the summer of 1974 using the Goddard Laboratory for Atmospheric Sciences general circulation model (GCM); a synoptic analysis for the month of July has shown that the behavior and structure of the simulated disturbances were similar to those observed with, in particular, the intensification of the waves just south of Lake Chad (for waves already formed somewhere in the east). Reed et al. (1988a,b) have evaluated the performance of the European Centre for Medium-Range Weather Forecasts (ECMWF) system in analyzing and forecasting (up to 48 h) the easterly waves; the simulated waves appeared to be slower than those analyzed. Druyan and Hall (1994) have determined the model representation of the waves in summer simulations of the Goddard Institute for Space Studies GCM.

The wave characteristics were realistic except for the phase speed, which was too slow as in the previous study. However, the simulated wave amplitude decreases too much in September compared to observations, and the precipitation was enhanced east of the wave trough contrary to observational evidence.

The aim of this study is to determine the ability of the Centre National de Recherches Météorologiques (CNRM) GCM to reproduce the space–time variability of the AEWs, with the help of two complementary objective methods [a space–time spectral analysis, hereafter called STSA, and a complex empirical orthogonal functions (CEOF) analysis, hereafter called CEOFA]. This validation study has been carried out using the ECMWF analyses as the reference (for the years 1982–88). Thus, the space–time variability of the AEWs as seen in the analyses will be discussed first, before the validation process itself (i.e., GCM simulation against ECMWF analysis).

This work is a preliminary study to precipitation monthly forecasts insofar as easterly waves are the smallest dynamical phenomena (which modulate rain-bringing systems and might be modulated by lower-frequency oscillations) that might be simulated by the model. Indeed, it is necessary to determine if the GCM is able to reproduce statistically the easterly wave space–time variance (with its interannual and intraseasonal variability) before testing the prediction ability (i.e., the capacity to reproduce the phase and amplitude evolution). The prediction hope is related to the low-frequency modulation of the easterly wave amplitude, exhibited in this paper.

After a discussion of the data and methods used in this study in section 2, the results obtained with the help of STSA (CEOFA) will be presented in section 3 (section 4), followed by the conclusions in section 5.

2. Data and methods

a. Data

The data used in this study are, on the one hand, the ECMWF analyses, widely described and used in many reports or papers [see ECMWF (1988) for a complete review], and, on the other hand, simulated data provided by the CNRM GCM integrated over the Atmospheric Model Intercomparison Project (AMIP) period, namely, 1979–88. The simulation was performed using observed sea surface temperature and observed ice pack extension on a monthly basis in the AMIP context (Gates 1992).

The version of the GCM (so-called Emeraude) used for the AMIP experiment is a spectral model with a T42 triangular truncation in the horizontal and an L30 discretization for the vertical, including 21 levels in the troposphere. This model includes a classic set of physical parameterizations such as radiative processes, convection using a mass flux scheme, and surface processes (Mahfouf 1993).

Looking at the climatology of the model, one may assume a rather good simulation of the summer monsoon flows in the Northern Hemisphere. However, focusing over West Africa, a northward shift of rainfall has been noticed (not shown). This discrepancy is linked to problems of surface processes representation (more precisely, albedo values that are too low over Sahara and sub-Sahara regions) and feedback effects between physical and dynamical processes. The albedo field has been improved since then.

Concerning ECMWF analyses, as mentioned by Duvel (1990), they are probably a better basis for GCM validation than local measurements as well as the best available information over regions with a poor observational network. The major problems in the use of such a dataset over a long period like that of AMIP are revisions of the analysis scheme, resolution changes, or parameterization improvements. A major change in the analysis scheme occurred in May 1984 (Shaw et al. 1987). A complete review of ECMWF parameterization changes has been done by Tiedke et al. (1988), including one of the most important changes introduced in May 1985. This change introduced the shallow convection, a revision of deep convection, a new cloud cover scheme, and an increase of the horizontal resolution (from T63 to T106). Finally, the use of divergent constraint in the analysis increments has been implemented in the wind analyses in January 1988.

The effects of the change implemented in May 1984 are not clearly documented for tropical regions. Nevertheless, one can expect, on one hand, a better accuracy of the analyzed winds since 1984 and, on the other hand, as highlighted by Shaw et al. (1987), less impact in the lower than in the upper troposphere.

Before the major change of May 1985, the main forecast errors (Tiedke et al. 1988) were a drying of the tropical troposphere, a cooling of the tropical troposphere, a weakening of the Hadley circulation, a weakening of subtropical highs, and a poleward and upward displacement of subtropical jets. Forecasts benefitted much from these parameterization and resolution changes. However, the differences in the wind analyses were quite modest (Tiedke et al. 1988), particularly looking at the low levels. The main modifications were a slight strengthening of the trade winds and an increase of convergence near the ITCZ.

Finally, the change of January 1988 (Unden 1989) seemed to have a low impact on vorticity, which will be the main parameter for our study.

Thus, we consider that the wind analyses are quite homogeneous and have a rather good quality over the period 1982–88, which enables us to use them as “references” in order to validate the results from the GCM. One can notice (Lare and Nicholson 1994) that these seven years are very different regarding rainfall over West Africa and the global interannual variability (El Niño/La Niña years).

The data were extracted every 6 h, using the ECMWF

FA leads to a decomposition of a space–time signal in the following form:

$$X(M, t) = \sum_{j=1}^p A_j(M)B_j(t) \cos(\omega_j t + k_{j,x}X + k_{j,y}Y),$$

where

$X(M, t)$ is the space–time signal,

M is the space variable corresponding to the zonal (X) and meridional (Y) directions,

t is the time variable,

$A_j(M)$ is the module of the CEOF j (CEOF n° j),

$B_j(t)$ is the module of the complex principal component j (CPC n° j),

$\omega_j = 2\pi/T_j$ is the pulsation of the CPC n° j (corresponding to the period T_j),

$\omega_j t = \varphi_j(t)$ represents the time phase of the CPC n° j ,

$k_{j,x} = 2\pi/\lambda_{j,x}$ corresponds to the zonal wavenumber of the CEOF n° j ,

$k_{j,y} = 2\pi/\lambda_{j,y}$ corresponds to the meridional wavenumber of the CEOF n° j , and

$k_{j,x}X + k_{j,y}Y = \Phi_j(M)$ represents the space phase of the CEOF n° j .

Looking at a traveling wave $X(M, t) = A(M)B(t) \cos[\varphi(t) + \Phi(M)]$ as a matter of evidence, the previous decomposition is particularly relevant for this kind of phenomenon.

To compute CEOFs, one can use two different methods. The first one uses the Hilbert's transform (Barnett 1983). This leads one to use a complex form of the real signal and consequently to compute the complex covariance matrix of the complex signal. CEOFs are given by eigenvectors (and associated eigenvalues) of the complex covariance matrix.

The second way, corresponding to the method proposed by Wallace and Dickinson (1972), uses time cross-spectrum computations. Then, integrating the cross-spectrum matrix over frequencies, we can obtain the complex covariance matrix. The different methods have been compared in Déqué (1986), and we chose to compute CEOFs using the cross-spectrum matrix. More precisely, we calculated the cross-spectrum using a sample method taking into account some advantages highlighted by Déqué (1986). So, we have split the six months of observations per year in eight samples corresponding to 92 observations each, that is to say, 23 days by sample (four observations per day). The length of each sample has been chosen considering the characteristic periods of AEWs (around 4 days) and the problems linked to the Fourier decomposition (namely, we must have enough periods in each sample in order to have a rather good estimation of the waves).

As recommended by Déqué (1986), we weighted data at each grid point taking into account the spherical surface of the domain. This led us to introduce a weight

that is proportional to the root of the cosine of the latitude.

Just before applying the CEOFA method, we used a classic empirical orthogonal function analysis (EOFA), in order to provide an easier calculation of CEOFs and to look at the ability of this factorial method to identify AEWs. Additionally, we made some sampling sensitivity tests both in space and time domains. Looking at the sensitivity of the methods to the space domain, we tested four different domains. One can see in Figs. 4a and 4b that the patterns of EOFs are quite stable from the larger domain (used for STSA) to the smaller one (finally retained for EOFA and CEOFA). In fact, the main differences between different analyses done are in the rank and percentage of variance corresponding to associated eigenvalues.

In the same way, results from raw and filtered data are also quite comparable both in space (for EOFs and CEOFs, not shown here) and time domains [for principal components (PCs) and CPCs]. As shown in Figs. 5a and 5b, the main difference came from the smoothing effect of the filter in the time domain. It has been noticed that the space phases (not shown here) are less noisy for filtered data.

3. Results from the space–time spectral analysis

a. Wave spectra

Figure 6 shows the space–time spectra (the all-space domain and May–October 1985) of the traveling waves for ECMWF (top panel) and the GCM (bottom panel). These diagrams give the power density versus the frequency (negative for eastward propagating phenomena) in the abscissa and the zonal wavenumber in the ordinate. On both spectra, there are several maxima of power density between 36 and 60 in time (3–5 days) for westward propagating phenomena and 2 and 4 in space (2200–4400 km). This spectral window is consistent with what has been found by other authors (e.g., Reed et al. 1988b) for the AEWs. However, the model variance maxima tend to be located toward lower frequency compared to the analysis variance maxima. Indeed, the secondary maximum of power density around 37 (5 days) is larger in the spectrum of the simulated data (Fig. 6). The order of magnitude of the model variance cumulated in the AEW spectral window is the same as that of the analysis variance (this topic will be discussed in more detail in section 4). Interestingly, there are also local maxima on both spectra for much lower frequencies of around ± 5 in time (37 days, for eastward and westward propagating oscillations) and for the first wavenumber. The same spectra computed for standing plus traveling waves (not shown) allow us to say that traveling wave variance represents 23% of the variance of all the waves, but more than 70% of the AEW variance. We have noticed the same kind of pattern for the other years, indicating a good similarity between anal-

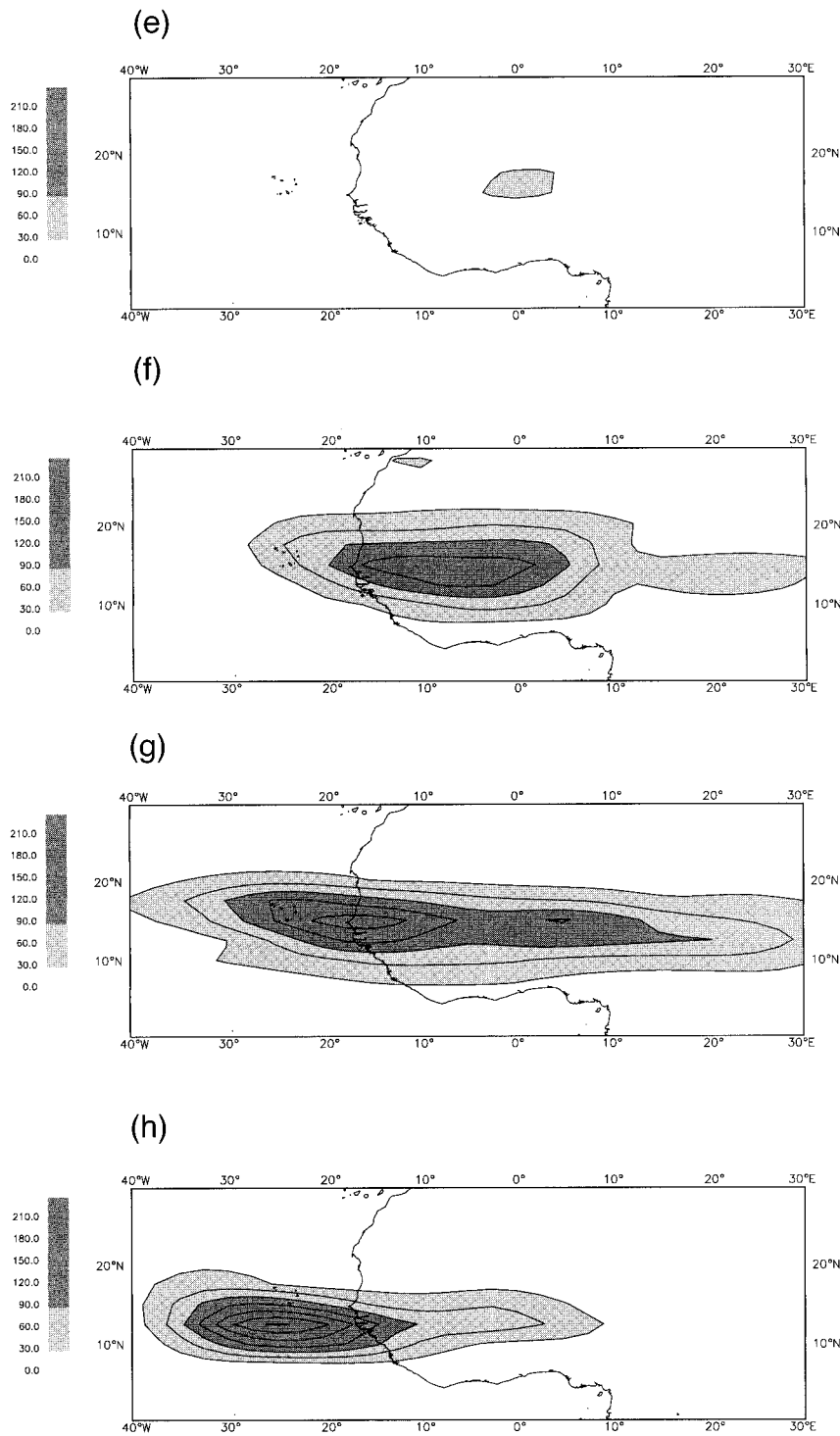


FIG. 8. (Continued)

over West Africa (see next section) strengthens the following interpretation: the northern single-track mode (i.e., mode 1) should be preferentially representative for AEWs associated with dynamical effects (i.e., with a predominant northerly component), while the dual-track

mode (i.e., mode 2) should catch the majority (in comparison with mode 1) of the AEWs associated with diabatic effects. In other words, the dual-track mode composes the majority of the AEWs characterized by a significant southerly component but also some AEWs char-

- Duvel, J. P., 1990: Convection over tropical Africa and Atlantic Ocean during northern summer. Part II: Modulation by easterly waves. *Mon. Wea. Rev.*, **118**, 1855–1868.
- ECMWF, 1988: Data assimilation and the use of satellite data. *ECMWF Seminar Proceedings*, Vol. 1, Reading, United Kingdom, ECMWF, 314 pp.
- Estoque, M. A., J. Shukla, and J. G. Jiing, 1983: African wave disturbances in a general circulation model. *Tellus*, **35A**, 287–295.
- Gates, W. L., 1992: AMIP: The Atmospheric Model Intercomparison Project. *Bull. Amer. Meteor. Soc.*, **73**, 1962–1970.
- Hastenrath, S., 1991: *Climate Dynamics of the Tropics*. Kluwer Academic, 488 pp.
- Hayashi, Y., 1977: On the coherence between progressive and retrogressive waves and a partition of space time power spectra into standing and traveling parts. *J. Appl. Meteor.*, **16**, 368–373.
- , 1979: A generalized method of resolving transient disturbances into standing and traveling waves by space-time spectral analysis. *J. Atmos. Sci.*, **36**, 1017–1029.
- , 1982: Space time spectral analysis and its applications to atmospheric waves. *J. Meteor. Soc. Japan*, **60**, 156–171.
- Horel, J. D., 1984: Complex principal component analysis: Theory and examples. *J. Climate Appl. Meteor.*, **23**, 1660–1673.
- Jenkins, G. M., and D. G. Watts, 1968: *Spectral Analysis and Its Applications*. Holden-Day Series, 517 pp.
- Lare, A. R., and S. E. Nicholson, 1994: Contrasting conditions of surface water balance in wet years and dry years as a possible land surface–atmosphere feedback mechanism in the West African Sahel. *J. Climate*, **7**, 653–668.
- Mahfouf, J. F., 1993: L'expérience d'intercomparaison AMIP: Simulation du climat 1979–1988 avec le modèle Emeraude. Note de travail du groupe de météorologie de grande échelle et climat 18, 32 pp. [Available from Météo-France—CNRM/GMGEC, F31057 Toulouse, France.]
- Mass, C., 1979: A linear primitive equation model of African wave disturbances. *J. Atmos. Sci.*, **36**, 2075–2092.
- Murakami, M., 1979: Large-scale aspects of deep convective activity over the GATE area. *Mon. Wea. Rev.*, **107**, 994–1013.
- Nitta, T., and Y. Takayabu, 1985: Global analysis of the lower tropospheric disturbances in the tropics during the northern summer of the FGGE year. Part II: Regional characteristics of the disturbances. *Pure Appl. Geophys.*, **123**, 272–292.
- Norquist, D. C., E. E. Recker, and R. J. Reed, 1977: The energetics of African wave disturbances as observed during the phase III of GATE. *Mon. Wea. Rev.*, **105**, 334–342.
- Paradis, D., J.-P. Lafore, J.-L. Redelsperger, and V. Balaji, 1995: African easterly-waves and convection. Part I: Linear simulations. *J. Atmos. Sci.*, **52**, 1657–1679.
- Payne, S. W., and M. M. McGarry, 1977: The relationship of satellite convective activity to easterly waves over West Africa and the adjacent ocean during phase III of GATE. *Mon. Wea. Rev.*, **105**, 413–420.
- Reed, R. J., D. C. Norquist, and E. E. Recker, 1977: The structure of African wave disturbances as observed during phase III of GATE. *Mon. Wea. Rev.*, **105**, 317–333.
- , A. Hollingsworth, W. A. Heckley, and F. Delsol, 1988a: An evaluation of the performance of the ECMWF operational system in analyzing and forecasting easterly wave disturbances over Africa and the tropical Atlantic. *Mon. Wea. Rev.*, **116**, 824–865.
- , E. Klinker, and A. Hollingsworth, 1988b: The structure and characteristics of African easterly wave disturbances as determined from the ECMWF operational analysis/forecast system. *Meteor. Atmos. Phys.*, **38**, 22–33.
- Rennick, M. A., 1976: The generation of African waves. *J. Atmos. Sci.*, **33**, 1955–1969.
- Saloum, M., 1993: Analysis of rain producing systems over Sahel region during the wet and dry period. *Proc. First Int. Conf. of African Meteorological Society*, Nairobi, Kenya, African Meteorological Society, 122–138.
- Shaw, D. B., P. Lönnberg, A. Hollingsworth, and P. Undén, 1987: Data assimilation: The 1984/85 revisions of the ECMWF mass and wind analysis. *Quart. J. Roy. Meteor. Soc.*, **113**, 533–566.
- Shove, D. J., 1946: A further contribution to the meteorology of Nigeria. *Quart. J. Roy. Meteor. Soc.*, **72**, 105–110.
- Thorncroft, C. D., and B. J. Hoskins, 1994a: An idealized study of African easterly waves. I: A linear view. *Quart. J. Roy. Meteor. Soc.*, **120**, 953–982.
- , and —, 1994b: An idealized study of African easterly waves. II: A nonlinear view. *Quart. J. Roy. Meteor. Soc.*, **120**, 983–1015.
- Tiedke, M., W. A. Heckley, and J. Slingo, 1988: Tropical forecasting at ECMWF: The influence of physical parameterization on the mean structure of forecasts and analyses. *Quart. J. Roy. Meteor. Soc.*, **114**, 639–664.
- Toledo Machado, L. A., J. P. Duvel, and M. Desbois, 1993: Diurnal variations and modulation by easterly waves of the size distribution of convective cloud clusters over West Africa and the Atlantic Ocean. *Mon. Wea. Rev.*, **121**, 37–49.
- Undén, P., 1989: Tropical data assimilation and analysis of divergence. *Mon. Wea. Rev.*, **117**, 2495–2517.
- Walker, J., and P. R. Rowntree, 1977: The effect of soil moisture on circulation and rainfall in a tropical model. *Quart. J. Roy. Meteor. Soc.*, **103**, 29–46.
- Wallace, J. M., and R. E. Dickinson, 1972: Empirical orthogonal representation of time series in the frequency domain. Part I: Theoretical considerations. *J. Appl. Meteor.*, **11**, 887–892.